

21ST INTERNATIONAL WORKSHOP ON RADIATION IMAGING DETECTORS
7–12 JULY 2019
CRETE, GREECE

A new physical model of Geiger-mode avalanche photodiodes

F. Ahmadov,^{a,c,1} F. Abdullayev,^a G. Ahmadov,^{a,b} R. Akbarov,^{b,c} R. Mukhtarov,^e S. Nuriyev,^{b,d}
A. Sadigov,^{b,c} Z. Sadygov,^{b,d} and S. Suleymanov^a

^aCenter for Strategic Scientific Research of ANAS,
Istiglaliyyat str. 30, AZ1001 Baku, Azerbaijan

^bJoint Institute for Nuclear Research,
Joliot-Curie 6, 141980 Dubna, Russia

^cNational Nuclear Research Centre of MTCHT,
Inshaatchilar 4, AZ1073 Baku, Azerbaijan

^dInstitute of Radiation Problems of ANAS,
B. Vahabzade 9, AZ1143 Baku, Azerbaijan

^eNational Aviation Academy,
Vill. Bina, AZ1045 Baku, Azerbaijan

E-mail: farid-akhmedov@yandex.ru

ABSTRACT: A new physical model of avalanche process with single photon detection capabilities is presented. The model describes the avalanche process, taking into account the resistance of space charge, parasitic capacitance as well as the changes of electric field during avalanche process caused by internal discharge and external recharge currents. The results of simulation are compared with the experimental data obtained with photodiodes from different manufacturers. It was determined that at a fixed value of overvoltage, the signal gain decreases significantly, depending on the resistance of the space charge region. This paper presents also the possibilities for improving the parameters of silicon photomultipliers.

KEYWORDS: Gamma camera, SPECT, PET PET/CT, coronary CT angiography (CTA); Photon detectors for UV, visible and IR photons (gas) (gas-photocathodes, solid-photocathodes); Photon detectors for UV, visible and IR photons (solid-state) (PIN diodes, APDs, Si-PMTs, G-APDs, CCDs, EBCCDs, EMCCDs, CMOS imagers, etc); Solid state detectors

¹Corresponding author.

Contents

1	Introduction	1
2	Modeling of the avalanche process	1
3	Experimental results and discussion	3
4	Conclusion	6

1 Introduction

In recent years, many researchers have studied the behavior of avalanche photodiodes under over-voltage conditions both theoretically and experimentally [1–3]. It has been a long time since the single-photon avalanche photodiode (SPAD) was proposed. However, no one has taken into account the effect of space charge resistance (R_s) on the characteristics of the SPAD devices. Currently, most users of micro-pixel avalanche photodiodes (MAPDs), named also as silicon photomultipliers (SiPMs), consider that the effective capacitance C_{eff} calculated as the slope of the single electron charge vs. voltage dependence is equal to the terminal capacitance C_p of the pixel (i.e., $C_{\text{eff}} \approx C_p$). However, in the paper [4] shown that this is not so, and in fact, $C_{\text{eff}} \approx 2 \times C_p$ in the case of very low space charge resistance ($R_s \approx 0$). As a result, the single electron charge is equal to $Q = C_p \times 2\Delta U_{\text{ov}}$, where $\Delta U_{\text{ov}} = U_d - U_b$ is the overvoltage value, U_d is bias voltage and U_b is breakdown voltage of the pixel. Actually, it is known that R_s is not equal to zero and varies in the range from tens of ohms to several kilo ohms depending on the structure design and size of the photodiodes [3]. In this work, we study the influence of R_s on the performance of SPAD devices and the possibilities of improving the parameters of Geiger-mode avalanche photodiodes as well as silicon photomultipliers.

2 Modeling of the avalanche process

A physical model for description the avalanche process in SPAD and MAPD photodetectors was developed in [5]. It is assumed that an MAPD pixel, as well as an SPAD device has a $p^+ - i - n^+$ structure with its terminal capacitance C_p and an individual quenching micro-resistor R_p . A new model of operation of Geiger-mode avalanche photodiodes mode is presented in figure 1. The new model of operation of Geiger-mode avalanche photodiodes contains an additional element — an ideal “spark gap” having no capacitance. Here the space charge resistance R_s and parasitic capacitance C_q shunting the quenching micro-resistor R_q are also taken into account.

Reverse bias voltage U_d applied to the pixel creates in the i -layer of thickness W a uniform electric field $E = E_0 = U_d/W$ strong enough to start the avalanche process. A single photo electron created within the i -layer near the pixel’s anode (p^+ -layer) creates electron-hole pairs on its way through entire thickness of the i -layer. Due to the exponential character of avalanche process, the

majority of these electron-hole pairs are created near the cathode (n^+ -layer, figure 1a). The same behavior is followed in avalanche processes initiated by a single hole. In last stage, the majority of electron-hole pairs are created near the pixel's anode (p^+ -layer). This circumstance leads us to make a model assumption that the impact ionization process takes place only in thin layers near the cathode and anode of the pixel (i.e. $d \ll W$). The gain factor for a single electron and a single hole was calculated as $M_e = \exp(\alpha W)$ and $M_h = \exp(\beta W)$, respectively. Here α and β are ionization coefficients for electrons and holes. The following expressions were used to take into account dependence of α and β on the electric field [6]:

$$\alpha(E) = 3.8 \times 10^6 \times \exp\left(-\frac{1.75 \times 10^6}{E}\right), \quad \beta(E) = 2.25 \times 10^7 \times \exp\left(-\frac{3.26 \times 10^6}{E}\right) \quad (2.1)$$

The number of electrons N_1 collected at the cathode, the number of holes P_{02} moving toward the anode, and the electric field E_1 during this stage can be expressed as $N_1 = \exp(\alpha_1 W)$, $P_{02} = [\exp(\alpha_1 W) - 1]$ and $E_1 = (U_{g1}/W)$, where $\alpha_1 = \alpha(E = E_1)$ and U_{g1} is the value of U_g (voltage drop on the “spark gap”) after the first avalanche stage. The holes with quantity P_{02} move towards the anode and create near it new electron-hole pairs after the time of $\tau = W/v_s$, where $v_s \approx 10^7$ cm/sec is the maximal drift velocity of charge carriers in silicon. All these holes are collected at the anode and a new number of electrons $N_{02} = [\exp(\alpha_1 W) - 1] \times [\exp(\beta_1 W) - 1]$ start the second stage of the avalanche process, where $\beta_1 = \beta(E = E_1)$. And so, new electrons appear near the anode after each time period 2τ , starting a new stage of the avalanche. As a result, the number of electrons collected at the cathode after the second stage of avalanche process is

$$N_2 = N_{02} \times \exp(\alpha_2 W) = [\exp(\alpha_1 W) - 1] \times [\exp(\beta_1 W) - 1] \times \exp(\alpha_2 W) \quad (2.2)$$

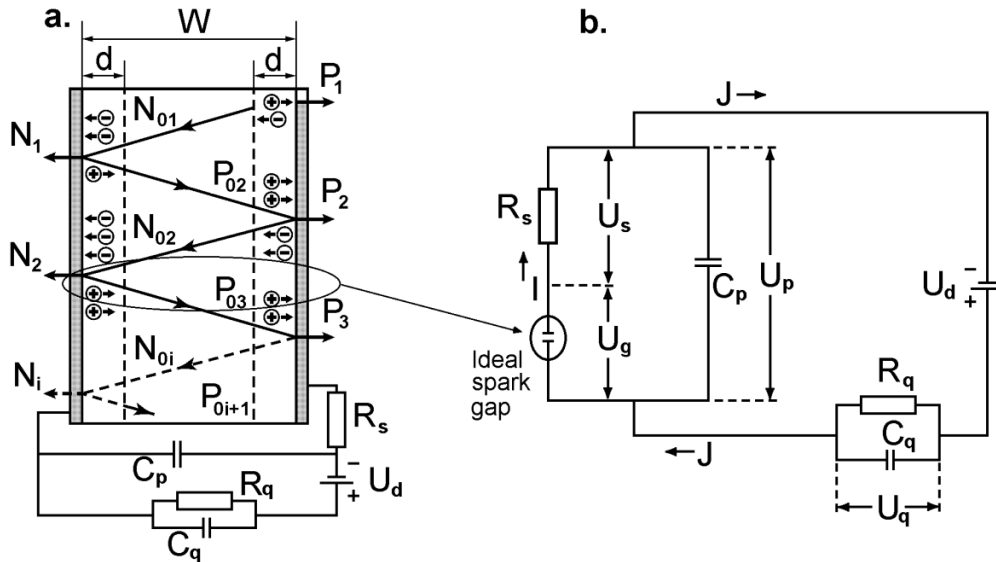


Figure 1. The physical model of performance (a) and the proposed equivalent circuit of the Geiger-mode avalanche photodiode (b).

Accordingly, the number of electrons collected at the cathode after the i -th stage is

$$N_i = \prod_{i=2}^n \{[\exp(\alpha_{i-1}W) - 1] \times [\exp(\beta_{i-1}W) - 1]\} \times \exp(\alpha_i W), \quad (2.3)$$

Full number of electrons (gain) after the i -th stage is expressed as $M = N_1 + \sum_{i=2}^n N_i$. Applying the Kirchhoff rules in the proposed new equivalent circuit, we can receive the following expressions for both the internal discharge current I_i and the external recharge current J_i :

$$I_i = qN_i/(2\tau); J_i = \frac{C_p(U_d - U_{gi})}{(C_p + C_q)R_q} - \frac{qC_pR_sN_{i-1}}{R_q(C_p + C_q) \times 2\tau} + \frac{qN_{i-1}}{2\tau} \times \left(\frac{C_q}{C_p + C_q} \right) \quad (2.4)$$

where $U_{gi} = U_d - U_{qi} - U_{si} = U_{g(i-1)} + \frac{U_d - U_{g(i-1)}}{(C_p + C_q)R_q} \times 2\tau - \frac{qN_{i-1}R_s}{(C_p + C_q)R_q} - \frac{qN_{i-1}}{C_p + C_q} - R_s \times \frac{q(N_i - N_{i-1})}{2\tau}$ and q — the electron charge.

3 Experimental results and discussion

Two types of single-photon avalanche photodiodes (SPADs) from two manufacturers have been investigated. The first SPAD was an experimental sample from Zecotek Photonics Inc. (www.zecotek.com). The active (photosensitive) region was $34 \mu\text{m} \times 34 \mu\text{m}$, while the contact region of the photodiode was $120 \mu\text{m} \times 120 \mu\text{m}$. This SPAD sample was manufactured on the basis of an epitaxial silicon layer of $3 \mu\text{m}$ thick with n -type conductivity grown on the surface of an n -type silicon substrate with low resistivity ($\sim 10 \Omega \cdot \text{cm}$).

The second SPAD (the part number: SAP500S2) was from Laser Components Company (www.lasercomponents.com). This sample is based on a $p^+ - \pi - p^+ - n^+$ structure. The depletion region has a thickness of about $25 \mu\text{m}$ (according to the information from Laser Components Company). The active area of the sample was round shape with a diameter of $500 \mu\text{m}$.

The avalanche process in both photodiodes was quenched by an external serial resistor of $R_q = 100 \text{ k}\Omega$. The SPAD devices were powered by a Keithley 6487 picoammeter. A blue light emitting diode (the part number: LED450L) with wavelength $\lambda \approx 450 \pm 20 \text{ nm}$ was used to investigate the amplitude distribution of single photoelectron signals from SPAD devices [7]. The LED was powered by a Tektronix-AFG3022B pulse generator with a pulse width of 30 nsec .

The signal from SPAD is amplified by the amplifier (bandwidth — 80 MHz , gain — 35). The output of the amplifier was connected to a CAEN DT5720B desktop digital converter to measure the total charge of the photo signals initiated by single photoelectrons. In order to catch the full signal, the integration gate width for SPADs from Laser Components Company and Zecotek Photonics were selected as 1400 nsec and 200 nsec , accordingly. All measurements were carried out at the ambient temperature of 22°C .

The measured value of the terminal capacitance C_p of the SPAD sample from Zecotek Photonics Inc. was 0.9 pF . The value of C_p was measured around the breakdown voltage U_b . Figure 2a shows the dependence of the single photoelectron charge Q on the applied bias voltage U_d . It can be seen that at $R_s \approx 4.6 \Omega$, the results of simulation describe well the experimental data. The intersection point of the linear fit of the Q vs. U_d dependence with the axis was taken equal to the breakdown voltage. The effective pixel capacitance calculated using the expression $C_{\text{eff}} = \partial Q / \partial U_d$ was 1.7 pF , which is approximately twice the value of the measured terminal capacitance C_p . This

means that after quenching of the avalanche process, the pixel potential falls below the breakdown voltage by the overvoltage value ΔU_{ov} and in this case the maximum discharge potential (ΔU_{dis}) is $\Delta U_{dis} = U_d - U_{p.min} = 2 \times \Delta U_{ov}$, where $U_{p.min}$ — is the minimum value of the pixel potential ($U_p = U_s + U_g$) just after the avalanche quenched (figure 1b).

The measured value of the terminal capacitance C_p of the sample from Laser Components Company was 2.6 pF. Figure 2b shows the dependence of the single photoelectron charge on the applied bias voltage. The effective pixel capacitance was obtained as 3.13 pF by using the expression $C_{eff} = \partial Q / \partial U_d$. This value of C_{eff} is approximately 1.2 times higher than the measured terminal capacitance C_p of the pixel (i.e. $C_{eff} \approx 1.2 \times C_p$). This indicates that, when the avalanche process is quenched, the pixel potential only slightly falls below the breakdown voltage without reaching the value about ΔU_{ov} below U_b . This is due to the local nature of the one-electron avalanche process in the photodiode. It is necessary to take into account the fact that the area of the pixel itself is much larger than the cross section of the multiplication channel of single photoelectrons. Therefore, the resistance of the depletion layer existing under the multiplication channel of one photoelectron has a significant effect on the discharge process. The resistance of this part of the depletion layer in the device SAP500S2 can be calculated as follows [5, 6]:

$$R_s = \frac{W^2}{2 \times \varepsilon_s \times S_p \times v_s} \approx 60 k\Omega \times \left(\frac{W}{D}\right)^2 \quad (3.1)$$

where W — is thickness of the depletion region, ε_s — dielectric permittivity of silicon, D — diameter of the single-photoelectron multiplication channel, $S_p = (\pi \times D^2)/4$ — area of cross-section of the avalanche channel, $v_s \approx 10^7$ cm/sec — the maximal thermal drift velocity of charge carriers in silicon.

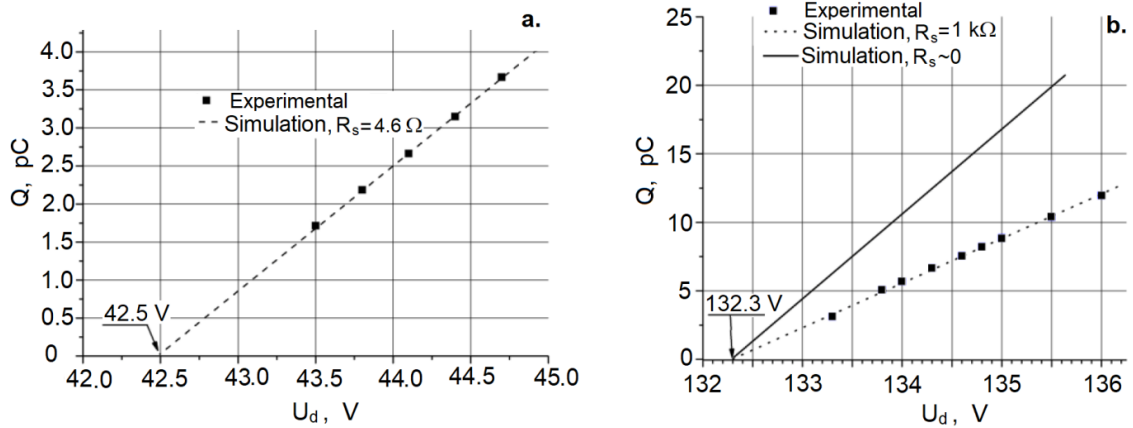


Figure 2. Full charge of single-photoelectron pulses as a function of the bias voltage applied to the SPAD sample from Zecotek Photonics Inc (a) and the SPAD device from Laser Components (b).

Figure 3a demonstrates the development of the internal discharge current I with time at an overvoltage $\Delta U_{ov} = 1$ V, a bias voltage $U_d = 133.3$ V and a breakdown voltage $U_b = 132.3$ V. It can be seen that at $R_s \approx 1 k\Omega$, the results of simulation describe well the experimental data (figure 2b). The maximum value of the internal current is 0.707 mA in the device SAP500S2 and that is why some

part of voltage drops on the resistor R_s of the depletion region: $I \times R_s = 0.707 \text{ mA} \times 1 \text{ k}\Omega \approx 0.71 \text{ V}$. In accordance with the expression (3.1), the value of $R_s \approx 1 \text{ k}\Omega$ corresponds to the value of the avalanche channel diameter $D \approx 194 \mu\text{m}$ in the device SAP500S2.

The dependence of the single photoelectron gain on R_s are shown in figure 3b. The maximum discharge potential (ΔU_{dis}) of the pixel decreases with increasing R_s . Therefore, the pixel gain M decreases with increasing R_s .

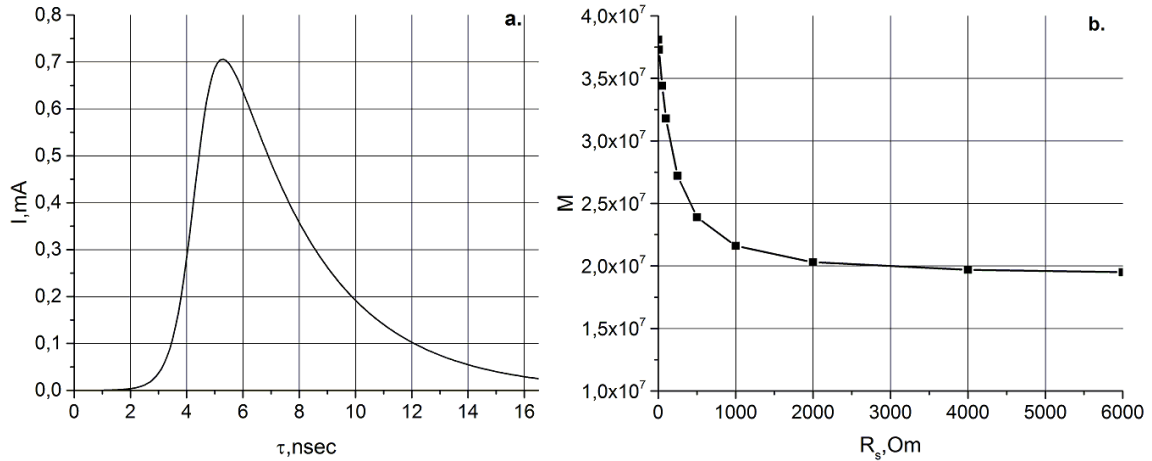


Figure 3. Time dependence of internal current (a. $U_d = 133.3 \text{ V}$, $R_s = 1 \text{ k}\Omega$) and the gain dependence of R_s (b. $U_d = 133.3 \text{ V}$) for the device from Laser Components Comp.

In this case, we propose to use the following expression to calculate the gain of SPAD and MAPD devices:

$$M = C_{\text{eff}} \times \Delta U_{\text{ov}} = m \times C_p \times \Delta U_{\text{ov}} \quad (3.2)$$

where ΔU_{ov} is the overvoltage, C_{eff} — the effective capacitance of the pixel containing also the parasitic capacitance C_q and equals $C_{\text{eff}} = m \times C_p$, m — is a coefficient which may change from 1 to 2 depending on the values of R_s , C_p and C_q .

Figure 4a presents the values of m vs. C_p . The value of m decreases with increasing the terminal capacitance C_p and reaches 1 when the terminal capacitance exceeds 3 pF (at fixed value of $R_s = 1 \text{ k}\Omega = \text{const}$). The value of m decreases with increasing R_s and it reaches 1 when $R_s > 3 \text{ k}\Omega$ (figure 4b).

The proposed model is also confirmed by the experimental results obtained in [8]. The authors of this paper showed that the signal amplitude of a single pixel of the MAPD (or MPPC) significantly increases depending of the number of photons incident on this pixel and at a pixel size of $50 \mu\text{m}$, the signal amplitude increases up to two times. In our opinion, this is explained by the fact that with an increase in the number of photons, the number of avalanche channels also increases and as a result, the resistance of the space charge R_s decreases. This leads to an increase in the amplitude of the signal according to the results shown in figure 4b.

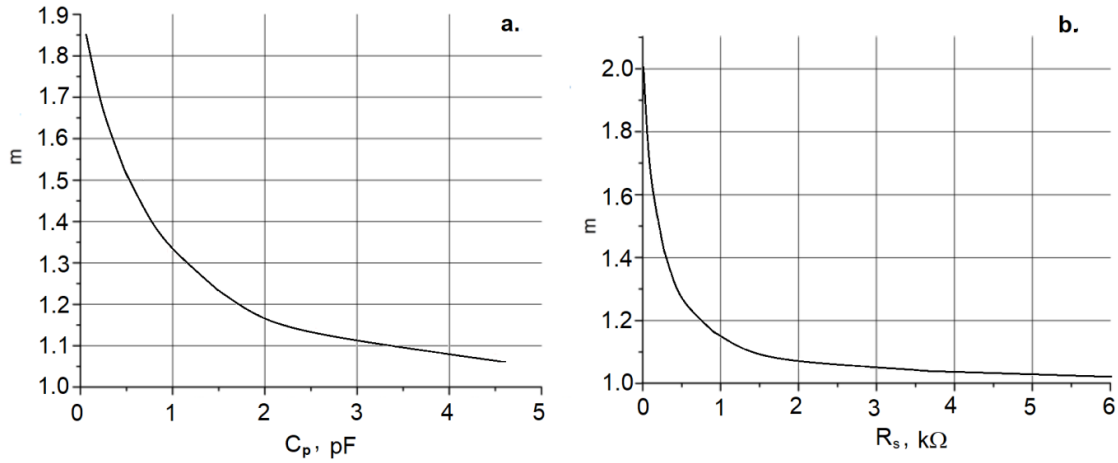


Figure 4. Dependence of the value of m on the terminal capacitance C_p and the resistance of the space charge region R_s : a. $\Delta U_{ov} = 1$ V, $R_s = 1$ k Ω ; b. $\Delta U_{ov} = 1$ V, $C_p = 3.13$ pF.

4 Conclusion

The single electron avalanche processes were investigated in SPAD samples from Zecotek Photonics Inc. and Laser Components Company. The effective pixel capacitance C_{eff} of the Zecotek's sample (calculated using the linear fit from Q vs. U_d dependence) is approximately two times higher than the value of the measured terminal capacitance C_p of the pixel.

In case of Laser Component's sample, the effective pixel capacitance C_{eff} is only 1.2 times higher than the measured terminal capacitance C_p of the pixel. In this case, the pixel potential slightly falls (about $0.2 \times \Delta U_{ov}$) below the breakdown voltage. This difference is due to a significantly voltage drop on the resistance R_s of a single photoelectron multiplication channel in the photodiode from Laser Component. The voltage dropped on this resistance was 0.707 V at 1 V overvoltage. Therefore, it can be concluded that the condition of $m = 2$ is an indicator of the optimal design of SPAD photodiodes aimed to maximise the gain for a given pixel capacitance and overvoltage.

A significant portion of the total capacitance $C_{tot} = C_p + C_q$ in SPAD detectors is contributed by the device's contact pad and by the parasitic capacitance C_q shunting the quenching resistor R_q . The discharge current increases with increasing pixel capacitance and in this case, the effect of the depleted layer resistance on the development of the avalanche process becomes more significant. Consequently, the minimal potential $U_{p,min}$ of the SPAD detector becomes close enough to the breakdown voltage U_b . This means that the avalanche process can continue and its quenching will acquire random (statistical) character. Stopping such an avalanche quickly necessitates either a large value of R_q (passive quenching element preventing significant charging of the device) or a dedicated electronic circuit ensuring a drop of the SPAD potential below the breakdown voltage U_b .

Unlike SPAD devices, the MAPD (or SiPM) pixel has tens of times smaller capacitance. This is why the resistance R_s of the depleted layer does not strongly affect the avalanche process and each pixel discharges down to a potential significantly below the breakdown voltage. This ensures quick quenching of the avalanche process in the MAPD pixel.

Acknowledgments

This work was supported by the Science Foundation of SOCAR.

References

- [1] R.H. Haitz, *Model for the electrical behavior of a microplasma*, *J. Appl. Phys.* **35** (1964) 1370.
- [2] S. Cova, A. Longoni and A. Andreoni, *Towards picosecond resolution with single-photon avalanche diodes*, *Rev. Sci. Instrum.* **52** (1981) 408.
- [3] S. Cova, M. Ghioni, A. Lacaita, C. Samori and F. Zappa, *Avalanche photodiodes and quenching circuits for single-photon detection*, *Appl. Opt.* **35** (1996) 1956.
- [4] A. Sadigov, F. Ahmadov, S. Suleimanov, N. Heydarov, R. Valiyev, M. Nazarov et al., *An Iterative Model of Performance of Micropixel Avalanche Photodiodes*, *Int. J. Adv. Res. Phys. Sci.* **3** (2016) 9 [<https://www.arcjournals.org/pdfs/ijarps/v3-i2/3.pdf>].
- [5] F. Ahmadov, F. Abdullayev, R. Akberov, G. Ahmadov, S. Khorev, S. Nuriyev et al., *On iterative model of performance of micropixel avalanche photodiodes*, *Nucl. Instrum. Meth. A* **912** (2018) 287.
- [6] S.M. Sze and K. Ng. Kwok., *Physics of Semiconductor Devices*, John Wiley & Sons, New York (2007).
- [7] <http://www.thorlabs.com/thorproduct.cfm?partnumber=LED450L>.
- [8] G. Kawata, K. Sasaki and R. Hasegawa, *Avalanche-area dependence of gain in passive-quenched single-photon avalanche diodes by multiple-photon injection*, *IEEE Trans. Electron Devices* **65** (2018) 2525.